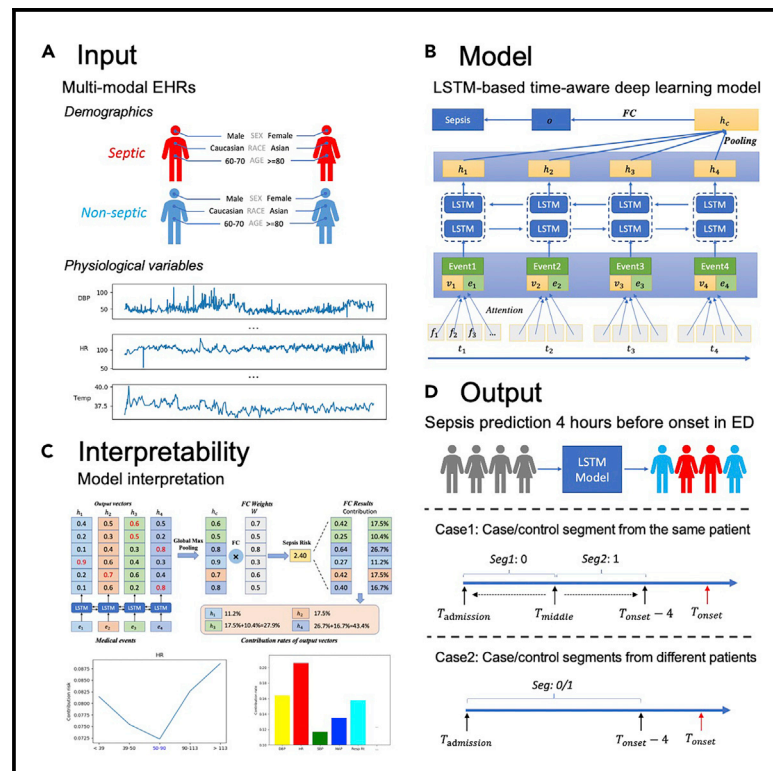


Patterns

An interpretable deep-learning model for early prediction of sepsis in the emergency department

Graphical Abstract



Authors

Dongdong Zhang, Changchang Yin, Katherine M. Hunold, Xiaoqian Jiang, Jeffrey M. Caterino, Ping Zhang

Correspondence

zhang.10631@osu.edu

In Brief

Electronic health records contain valuable temporal information for sepsis prediction. However, irregular time intervals between neighboring events are typically neglected. Besides, transparency and interpretability of deep-learning models with increasing complexity and superior performance has become a barrier to the models' clinical adoption. To this end, we propose an interpretable deep-learning model that better captures time information and achieves promising performance on sepsis prediction in the emergency department.

Highlights

- We present benchmark results of sepsis-onset prediction in emergency department
- An LSTM-based model captures irregular time intervals with time encodings
- Our deep-learning model shows superior performance compared with existing methods
- Model interpretation enables real-world clinical applications



Article

An interpretable deep-learning model for early prediction of sepsis in the emergency department

Dongdong Zhang,^{1,6} Changchang Yin,^{1,2,6} Katherine M. Hunold,³ Xiaoqian Jiang,⁴ Jeffrey M. Caterino,³ and Ping Zhang^{1,2,5,6,7,*}

¹Department of Biomedical Informatics, The Ohio State University, Columbus, OH 43210, USA

²Department of Computer Science and Engineering, The Ohio State University, Columbus, OH 43210, USA

³Department of Emergency Medicine, The Ohio State University, Columbus, OH 43210, USA

⁴School of Biomedical Informatics, The University of Texas Health Science Center, Houston, TX 77030, USA

⁵Translational Data Analytics Institute, The Ohio State University, Columbus, OH 43210, USA

⁶These authors contributed equally

⁷Lead contact

*Correspondence: zhang.10631@osu.edu

<https://doi.org/10.1016/j.patter.2020.100196>

THE BIGGER PICTURE Sepsis is the leading cause of death worldwide and has become a global epidemiological burden. Early prediction of sepsis enables early treatment and increases the likelihood of survival for septic patients. The broad adoption of electronic health records (EHRs) provides an opportunity for sepsis prediction. However, most existing prediction approaches do not consider irregular time intervals between neighboring clinical events in EHRs. Besides, many deep-learning models suffer from black-box problems and are not trusted in clinical settings. We propose a deep-learning model with time encodings, offering both high accuracy and high transparency as well as clinical interpretability. We have already made our code and its detailed documentations publicly available, enabling colleagues to apply it to their applications and eventually make clinical impacts.



Proof-of-Concept: Data science output has been formulated, implemented, and tested for one domain/problem

SUMMARY

Sepsis is a life-threatening condition with high mortality rates and expensive treatment costs. Early prediction of sepsis improves survival in septic patients. In this paper, we report our top-performing method in the 2019 DII National Data Science Challenge to predict onset of sepsis 4 h before its diagnosis on electronic health records of over 100,000 unique patients in emergency departments. A long short-term memory (LSTM)-based model with event embedding and time encoding is leveraged to model clinical time series and boost prediction performance. Attention mechanism and global max pooling techniques are utilized to enable interpretation for the deep-learning model. Our model achieved an average area under the curve of 0.892 and was selected as one of the winners of the challenge for both prediction accuracy and clinical interpretability. This study paves the way for future intelligent clinical decision support, helping to deliver early, life-saving care to the bedside of septic patients.

INTRODUCTION

Sepsis, a life-threatening illness caused by the body's response to an infection, is the leading cause of death worldwide and has become a global epidemiological burden. Sepsis occurs at all ages and increases mortality rates. In the United States, for example, over 1.7 million adults develop sepsis and nearly 270,000 patients die as a result of sepsis each year.¹ Besides, sepsis is the costliest among all disease states and accounted for \$24 billion of United States hospital costs in 2013.² Without

timely and adequate treatment, sepsis can progress to severe sepsis and septic shock, which lead to higher mortality rates.³ Several studies suggest that early prediction of sepsis enables early treatment and is able to significantly improve patient outcomes.^{4,5} However, common signs and symptoms of sepsis, such as fever, chills, rapid respiration, and high heart rate, are the same as in other conditions, making sepsis difficult to diagnose in its early stages. Besides, it is clinically meaningless to predict sepsis minutes before onset even with high prediction accuracy. A good predictive model should be able to trigger



alerts as early as possible and present increasingly stronger signals as it approaches the actual event.

Electronic health records (EHRs) are longitudinal electronic records of patients' health information. The rapid growth in volume and diversity of EHRs during the last decades makes it possible to apply machine-learning and data-mining methods to the early prediction of sepsis. Screening tools have been used clinically to recognize sepsis, including quick Sequential (Sepsis-Related) Organ Failure Assessment (qSOFA),⁴ Modified Early Warning Score (MEWS),⁶ National Early Warning Score (NEWS),⁷ and Systemic Inflammatory Response Syndrome (SIRS).⁸ However, those tools were designed to screen existing symptoms as opposed to explicitly predicting sepsis prior to its onset, and their efficacy in sepsis diagnosis is limited. For example, prior studies show that qSOFA had low sensitivities in identifying sepsis in both prehospital and emergency department (ED) settings.^{9,10}

With recent advances and success, machine-learning methods have shown great potential in unlocking insights from EHRs. Various methods have been developed for accurate sepsis prediction.^{11,12} Faisal et al.¹³ developed a logistic regression model (CARS) to predict the risk of sepsis using a patient's firstly recorded vital signs and blood test results, which are usually available within a few hours of emergency admission. Horng et al.¹⁴ constructed a machine-learning model using a linear support vector machine and demonstrated the incremental benefit of using free text data in addition to vital signs and demographic data for sepsis clinical decision support at the ED. Mollura et al.¹⁵ trained a bagged tree classifier using the recorded electrocardiogram and arterial blood pressure waveforms, showing that the waveform monitoring information may help in detecting sepsis within the first hour of stay in the intensive care unit (ICU). Kamaleswaran et al.¹⁶ showed that artificial intelligence can be used to predict the onset of severe sepsis as early as 8 h ahead using physiometers in critically ill children. Lyra et al.¹⁷ used an optimized random forest to predict sepsis for imbalanced clinical data from ICUs in the PhysioNet Computing in Cardiology Challenge 2019.¹² Mao et al.¹⁸ validated a machine-learning algorithm with gradient-boosting trees, *InSight*, which used only six vital signs for the prediction of sepsis, severe sepsis, and septic shock and showed that *InSight* outperformed existing sepsis-scoring systems. Using 65 features from a combination of EHRs and high-frequency physiological data, Nemati et al.¹⁹ developed and validated an interpretable machine-learning model based on a modified Weibull-Cox proportional hazards algorithm for making an accurate and interpretable prediction of sepsis. Recently, deep-learning methods have achieved improving performances over traditional models and have shown unprecedented potential in the healthcare domain.²⁰ Deep-learning models automatically learn the data representation with improved performance and do not require conventional feature-extraction steps. Recurrent neural networks (RNNs) are commonly used network architectures in modeling multivariate series prediction.^{21–23} Kam and Kim²¹ proposed a sepsis-detection model with long short-term memory (LSTM), which showed better performance than *InSight* and superior capability for sequential patterns. However, deep-learning models usually suffer from black-box problems and are not trusted in clinical settings. RETAIN²⁴ and Dipole²⁵ proposed to introduce attention mechanisms and interpret the models' output risks based on

the learned attention weights, which is helpful for models' application to real-world clinical settings.

Most existing approaches^{11,12,17,21} focus on the sepsis prediction for ICU settings and may suffer from performance decrease for predicting sepsis onset for patients in EDs with low resolution of medical observations, while many patients have been diagnosed with sepsis at ICU admission.²⁶ Moreover, most of the aforementioned existing methods do not or only consider the relative order of events and ignore the irregular time intervals between neighboring events while modeling time-series EHR data. Besides, the increasing complexity of deep-learning models has brought superior model performances at the price of lack of transparency and interpretability, which has become a barrier to the models' clinical adoption. To this end, we address these problems with our proposed interpretable LSTM-based deep-learning model that can achieve state-of-the-art sepsis-onset prediction in the ED.

Our proposed deep-learning model handles irregular time intervals with time encodings, and leverages attention mechanism and global max pooling techniques to help interpret the model's behavior. Our team, *BuckeyeAI*, participated in the 2019 DII challenge with the proposed deep-learning method and ranked second out of 30 teams on the early prediction of sepsis onset in the ED, with an average area under the receiver-operating characteristic curve (AUC) score of 0.892. The goal of the 2019 DII challenge is the early prediction of sepsis using a patient's demographic and physiological data in the ED. Different from the PhysioNet Computing in Cardiology Challenge 2019 on sepsis prediction in the ICU,¹² the 2019 DII challenge focused on sepsis prediction in the ED where the environment is more chaotic.²⁷ In this paper, we present our methods, results, and analyses. To summarize, the contributions are as follows.

- We present benchmark results of sepsis-onset prediction in the ED. We show that our model outperforms four early-warning scores and three baseline machine-learning models.
- We propose an LSTM-based model for sepsis-onset prediction, which handles irregular time intervals with time encodings.
- We leverage the attention mechanism and global max pooling techniques to help interpret our model.

RESULTS

Study design

Definition of Sepsis-2, the presence of proven or suspected infection together with two or more SIRS criteria,²⁸ is used to define ground truth in the ED. The inclusion and exclusion diagram of the 2019 DII challenge data preparation pipeline is shown in [Figure 1](#). A summary of patient characteristics is provided in [Table 1](#). Distribution of length of stay until sepsis onset is shown in [Figure S1](#). Two use cases of sepsis-onset prediction 4 h before it occurs is demonstrated in [Figure 2](#). The proposed deep-learning model's architecture is illustrated in [Figure 3](#). Our proposed model handles irregular time intervals with time encodings, and the model is interpretable due to the attention mechanism and global max pooling techniques.

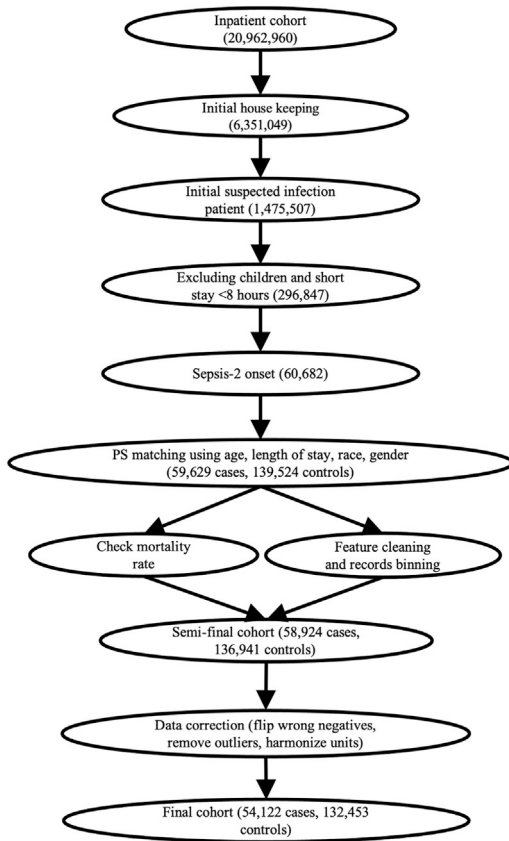


Figure 1. Inclusion and exclusion diagram of DII challenge data preparation pipeline

After filtering and correction, the final cohort has a sepsis prevalence of 29.0%.

We implemented and evaluated four early-warning scores, three traditional machine-learning methods, and four deep-learning models as baselines. The four early-warning scores comprised MEWS,⁶ NEWS,⁷ SIRS,⁸ and qSOFA.⁴ For traditional machine-learning methods, we considered logistic regression, random forest, and gradient-boosting trees. Because these standard machine-learning methods cannot work directly with multivariate time-series sequences, the element-wise aggregation (i.e., count, mean value, minimum value, maximum value, and standard deviation of events) of temporal features are used as model inputs. For the deep-learning baselines, two classical RNN models (i.e., GRU²⁹ and LSTM³⁰) and two state-of-the-art interpretable RNN models (i.e., RETAIN²⁴ and Dipole²⁵) are selected. The RNN models cannot handle the missing values of EHR data. We mapped the feature variables into vectors via an embedding layer. The concatenation of the embedding vectors and the observed feature values were then input to the RNN models.

Classification results

Table 2 summarizes the performance of various models for sepsis-onset prediction. From Table 2, our model outperforms baseline models. The main reasons why our model works better are 2-fold: (1) our model can automatically learn better patient

Table 1. Label statistics and characteristics of the final cohort

	Sepsis-2 patients (n = 52,802) (29.5%)	Sepsis-2 controls (n = 126,041) (70.5%)	Risk ratio
Gender			
Female	25,936 (49.1%)	65,523 (52.0%)	0.92
Male	26,866 (50.9%)	60,518 (48.0%)	1.08
Race			
African American	11,084 (21.0%)	20,556 (16.3%)	1.24
Asian	1,085 (2.1%)	1,627 (1.3%)	1.36
Caucasian	35,059 (66.4%)	95,657 (75.9%)	0.73
Others/unknown	5,574 (10.5%)	8,201 (6.5%)	1.41
Age			
18–20	1,602 (3.0%)	1,776 (1.4%)	1.63
20–40	8,100 (15.3%)	15,288 (12.1%)	1.20
40–60	15,654 (29.6%)	34,295 (27.2%)	1.09
60–80	20,241 (38.3%)	51,914 (41.2%)	0.92
80–100	7,205 (13.6%)	22,768 (18.1%)	0.78

representations as the network grows deeper and yield more accurate predictions with sufficient data; (2) our LSTM-based model can better capture temporal information, while logistic regression, random forest, and gradient-boosting trees simply aggregate time-series features and hence suffer from information loss.

We found that machine-learning-based algorithms outperformed early-warning scores on both cases. All three machine-learning methods achieved similar performance on both Case 1 and Case 2. MEWS and NEWS were shown to perform better than SIRS and qSOFA on Case 2. However, the result suggested little discrimination of four scores on Case 1 with low AUC scores. The deep-learning models outperformed the early-warning scores and performed comparably with the machine-learning algorithms. We speculate the reason for this is that the feature engineering (e.g., minimum and maximum feature values) is effective, and both machine-learning and deep-learning methods can capture the abnormal values from EHRs. With the help of attention mechanisms, RETAIN and Dipole can focus on the abnormal values better, and thus outperform GRU and LSTM.

On the private test dataset, our proposed model achieved AUC scores of 0.940 and 0.845 for two use cases, respectively. The official score is $(0.940 + 0.845) / 2 = 0.892$. Compared with attention-based models (i.e., RETAIN and Dipole), the proposed model still achieves better prediction accuracy. Our model considers the whole history of a patient's EHRs with a global pooling operation rather than attention, which is useful for relieving the long-term dependency problem of RNN. Moreover, the time embedding can capture the temporal information more efficiently, which further improves the proposed model's performance.

Ablation study

To measure the effectiveness of different components (i.e., event embeddings, time encodings, and global max pooling), we adopt an ablation study to gain a better understanding of the proposed model by removing one component each time. The results of

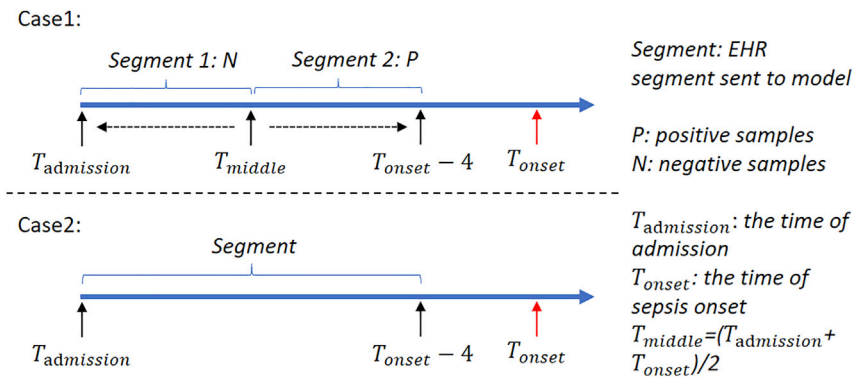


Figure 2. Two use cases of sepsis-onset prediction 4 h before it occurs

try to interpret our model at the population level in two ways, namely medical event importance and influential clinical features.

Medical event importance

As we can calculate the contribution rate of each medical event of each patient, we can compute each medical event's importance at the population level. For each medical

ablation study on Case 1 sepsis-onset prediction are reported in Table 3. Based on the results from Table 3, the most influential component is event embeddings. By removing event embeddings, the AUC score decreases by 0.11. By handling irregular time intervals using time encoding, the model performance increases from 0.89 to 0.94. Moreover, incorporating global max pooling causes an AUC score increase of 0.03.

DISCUSSION

Generally, linear models and tree-based models can be easily interpreted because of their intuitive way of predicting output from inputs, but these models are quite simple. Although deep-learning models can usually yield more accurate predictions, they usually operate as black boxes and make it unclear why the models make specific predictions. However, due to the attention mechanism and global max pooling operation, our deep-learning model is interpretable as shown in Figure 6. At patient level, we are able to calculate the contribution rate of each medical event for sepsis risk according to Equation 5. Medical events with higher contribution rates contribute most to the clinical outcome (i.e., sepsis onset in the next 4 h).

While patient-level interpretation reveals medical events that are most influential to sepsis onset for an individual patient, population-level analysis is needed to determine the most influential medical events as well as clinical features over the entire EHR dataset. Therefore, to better understand the model's behavior, we

event, event importance is calculated by averaging its contribution rates for all patients whose EHR data contain this event.

Figure 4 shows the medical event importance (average contribution rate) over time for all patients. This plot shows an overall upward trend, which meets our expectation that the medical events closer to sepsis onset are more important for our model to make predictions.

Clinical feature importance

Apart from medical event importance, we also want to know which clinical features are most important for sepsis-onset prediction. Similar to medical event importance, for each clinical feature we compute its importance over all medical events across the entire population according to Equation 6. The top influential features found by the deep-learning model are shown in Figure 5. The full contribution rate list of clinical features can be found in Table S1. The clinical features with the highest contribution to sepsis prediction are easily attainable clinical values. Thus, our model suggests that the development of sepsis can be predicted easily based on items within the EHR. Interestingly, lab values traditionally associated with sepsis prediction (e.g., white blood cell count and renal function) were not predictive.

Model performance across subpopulations

From this perspective, we compare the model performance across various subpopulations and report the results on

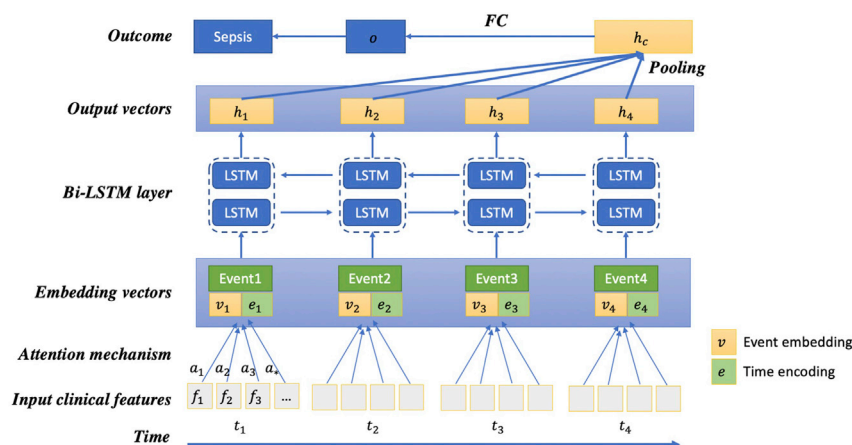


Figure 3. Architecture of proposed LSTM-based model

The concatenation of the medical event embedding vectors (v_1, v_2, \dots, v_n) and the corresponding time encoding vectors (e_1, e_2, \dots, e_n) are inputs to the BiLSTM model, which generates output vectors (h_1, h_2, \dots, h_n). All the output vectors are concatenated, then a global max pooling operation is performed to produce the patient representation vector. Finally, a fully connected layer and the sigmoid function are used to predict the probability of sepsis onset in the next 4 h.

Table 2. AUC scores of sepsis-onset prediction task

Method	Case 1	Case 2	Average
MEWS	0.54	0.72	0.63
NEWS	0.52	0.72	0.62
SIRS	0.56	0.69	0.62
qSOFA	0.53	0.65	0.59
Logistic regression	0.89	0.79	0.84
Random forest	0.90	0.81	0.85
Gradient-boosting trees	0.91	0.81	0.86
GRU	0.88	0.80	0.84
LSTM	0.89	0.80	0.85
RETAIN	0.90	0.80	0.85
Dipole	0.90	0.81	0.86
Proposed model	0.94	0.84	0.89

Case 1 sepsis prediction as an example in Table 4. The results show that our model achieves high prediction performance (AUC ≥ 0.929) across all subpopulations. Confidence intervals are calculated at the 95% level. We also test paired p values for model performance between subgroups, the results of which are reported in Table S2. Concerning gender, the model seems to perform better on female patients compared with male patients, with higher AUC scores ($p = 0.025$). For race subgroups, performance on the African American patients is the most discriminatory, with relatively lower p values compared with other combinations. The model's AUC on Asian patients is lower with large variance, perhaps because the proportion of Asian patients is small. With respect to age subgroups, the model achieves higher performance for patients whose age is lower than 20 years while the result shows large variance due to the low proportion of such patients. Model performances on patient pairs aged 20–30 and 30–40, 50–60, and 60–70 years are quite similar. The reason for this could be that the distributions of features of these pairs are closer.

Conclusion

Our team, *BuckeyeAI*, participated in the 2019 DII Challenge and ranked #2 out of 30 teams on the early prediction of sepsis onset task. In this paper, we present our solution to sepsis-onset prediction, our proposed deep-learning model achieved an AUC score of 0.892 and outperformed four early-warning scores and three baseline machine-learning models. By incorporating event embeddings,

Table 3. Ablation study of different components (i.e., event embeddings, time encodings, and global max pooling) on Case 1 sepsis prediction

Model	AUC
Proposed model without event embeddings	0.83
Proposed model without time encodings	0.89
Proposed model without global max pooling	0.91
Proposed model	0.94

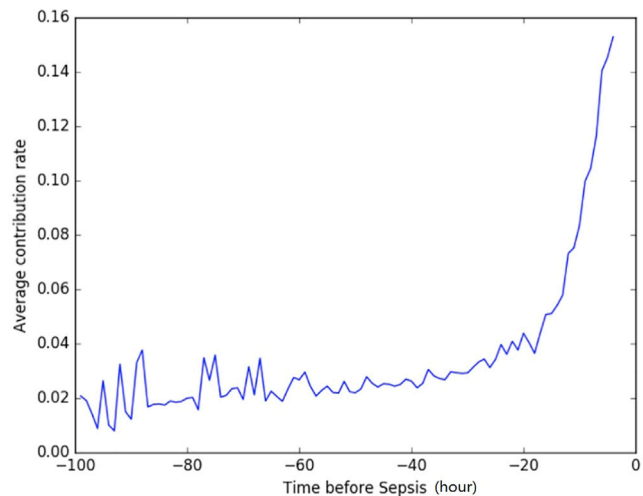


Figure 4. Average contribution rate of medical events over time for patients in test set

Note that when computing the average contribution rate for a specific time point, we only consider the patients who have medical events at the time point.

time encodings, and global max pooling, our model yields more accurate predictions. Time encodings help to handle irregular time intervals. The global pooling operation enables the model to associate the contribution of each medical event with the final clinical outcome, paving the way for interpretable clinical risk predictions.

Although we mainly focus on sepsis-onset prediction in this challenge, our model is general and can be applied to other multivariate time-series prediction problems. In addition to the superior performance, our proposed model is interpretable from an individual patient to the whole population.

EXPERIMENTAL PROCEDURES

Resource availability

Lead contact

Further information and requests for resources should be directed to and will be fulfilled by the Lead Contact, Ping Zhang, PhD (zhang.10631@osu.edu).

Materials availability

This study did not generate any new materials.

Data and code availability

Protected Health Information restrictions apply to the availability of the 2019 DII Challenge dataset. As a result, the dataset is not publicly available. The source code is provided and is available at <https://github.com/yingchangchang/DII-Challenge>.

Ethical statement

The challenge data are extracted from the Cerner Health Facts database. All challenge entrants signed an enforceable data use agreement as part of the competition registration process. Regarding the use of Cerner Health Facts, all challenge publications authors are covered under IRB protocol HSC-SBMI-13-0549, approved by the UT Health Committee for the Protection of Human Subjects.

Data

The challenge data are extracted from the Cerner Health Facts database. Cerner Health Facts is a database that comprises de-identified EHR data from over 600 participating Cerner client hospitals and clinics in the United

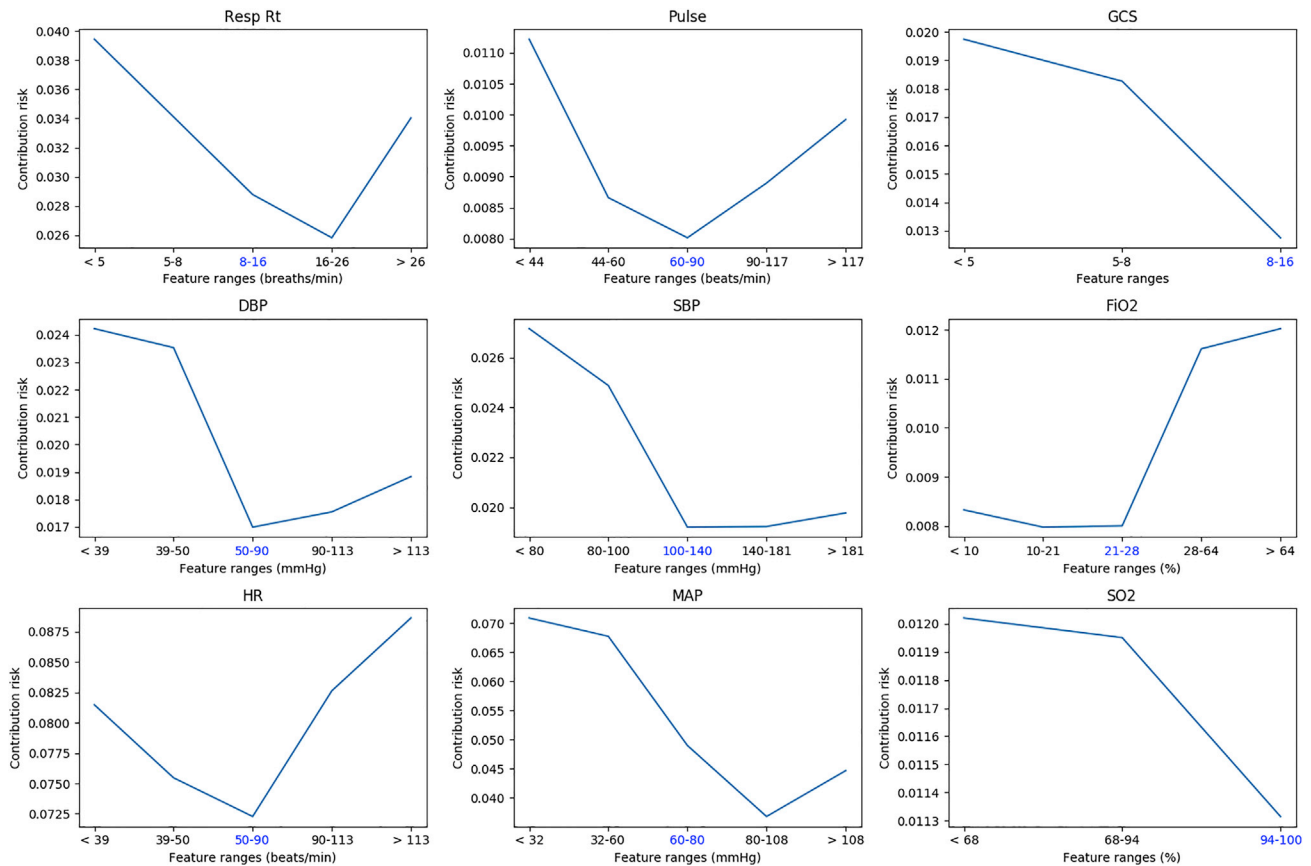


Figure 5. Contribution risks of top influential features found by the deep-learning model
Blue-colored tick label on x axis is the corresponding normal range of each feature.

States and represents over 106 million unique patients. With this longitudinal, relational database reflecting data from 2000 to 2016, researchers can analyze detailed sets of de-identified clinical data at the patient level. Types of data available include demographics, encounters, diagnoses, procedures, lab results, medication orders, medication administration, vital signs, microbiology, surgical cases, other clinical observations, and health systems attributes.

The goal of 2019 DII challenge is the early prediction of sepsis with demographic and physiological data provided. Sepsis-2 is diagnosed as the presence of proven or suspected infection together with two or more SIRS criteria. The SIRS criteria are defined as:

- Heart rate >90 beats/min
- Body temperature >38°C or <36°C
- Respiratory rate >20 breaths/min or PaCO₂ <32 mm Hg
- White blood cell count >12 × 10⁹ cells/L or <4 × 10⁹ cells/L

Sepsis-2 definition is used to define the ground truth. Patients who are <18 years old or do not have enough observation data are excluded. The whole data preparation pipeline diagram is shown in Figure 1. The label statistics and characteristics of the final cohort are provided in Table 1. Descriptions and statistics of clinical features are available in Table S1.

Predictive tasks

In this challenge, we aim to predict sepsis 4 h before onset for hospitalized adult patients. There are two use cases, as demonstrated in Figure 2.

Case 1

In this case, patients are sampled from septic patients, and the goal is to find out whether a model can tell if a patient is likely to have high sepsis risk a few

hours before the onset. For each patient, the patient records is split into two segments at the middle point, segment close to sepsis onset (= 4 h) is labeled as 1, another segment (>4 h before sepsis onset) is labeled 0. We randomly pick either the former or latter segment to build the Case 1 cohort. The introduction of case 1 is to measure the model in terms of time-sensitive prediction to ensure models are indeed clinically useful and relieve warning fatigue as alarm burden. Given patient records either from $T_{\text{admission}}$ to T_{middle} or from T_{middle} to $T_{\text{onset}} - 4$, our model is required to distinguish these two kinds of records.

Case 2

In this case, case and control segments are from different patients who have sepsis onset in the next 4 h, as well as those who do not have sepsis. Given patient records from $T_{\text{admission}}$ to $T_{\text{onset}} - 4$, we are going to predict whether sepsis occurs in the following 4 h.

Neural network architecture

The proposed neural network architecture is shown in Figure 3. This model is inspired by DG-RNN.³¹ Although we focus on the early prediction of sepsis onset in this challenge, our proposed model is general and can be applied to other multivariate time-series prediction tasks, such as mortality prediction for septic patients.

Event embeddings

For each temporal feature, we sort the values from low to high and use the order to replace the original values. We then divide the orders into ten groups (i.e., 0.0–0.1, 0.1–0.2, ..., 0.9–1.0) and each event is then embedded into a 512-day vector.

Table 4. Model performance (AUC) with 95% confidence interval across various subpopulations on Case 1 sepsis prediction

	AUC
Total	0.942 (0.938, 0.946)
Gender	
Female	0.946 (0.939, 0.953)
Male	0.938 (0.935, 0.941)
Race	
African American	0.950 (0.941, 0.959)
Asian	0.929 (0.894, 0.963)
Caucasian	0.937 (0.934, 0.941)
Others/unknown	0.933 (0.925, 0.941)
Age	
18–20	0.966 (0.949, 0.983)
20–30	0.933 (0.919, 0.946)
30–40	0.931 (0.923, 0.939)
40–50	0.947 (0.941, 0.953)
50–60	0.939 (0.933, 0.946)
60–70	0.940 (0.928, 0.952)
70–80	0.931 (0.921, 0.941)
80–100	0.947 (0.938, 0.955)

Time encodings

When modeling time-series EHR data, most existing LSTM-based models do not or only consider the relative order of events. However, these methods typically ignore the irregular time intervals between neighboring events. Similar to position encodings in Transformer,³² we infuse time information using time encodings. Time encodings are sent to LSTM together with event embeddings. We compute each event’s relative time to the criterion operation date and the time interval relative to the last event. We then use sine and cosine functions of the different time intervals to represent the time encoding for the t^{th} event:

$$\begin{aligned}
 p_{t,2j} &= \sin((date_o - date_t)/51200j/d) \\
 p_{t,2j+1} &= \cos((date_o - date_t)/51200j/d) \quad (Equation 1) \\
 0 \leq j < d
 \end{aligned}$$

where $date_o$ denotes the criterion operation date, $date_t$ denotes the t^{th} event’s date, $p_t \in R^{2d}$ denotes the time encoding vector, and j is the dimension of EHRs event embeddings. Both the event embeddings and time encodings are then input to LSTM.

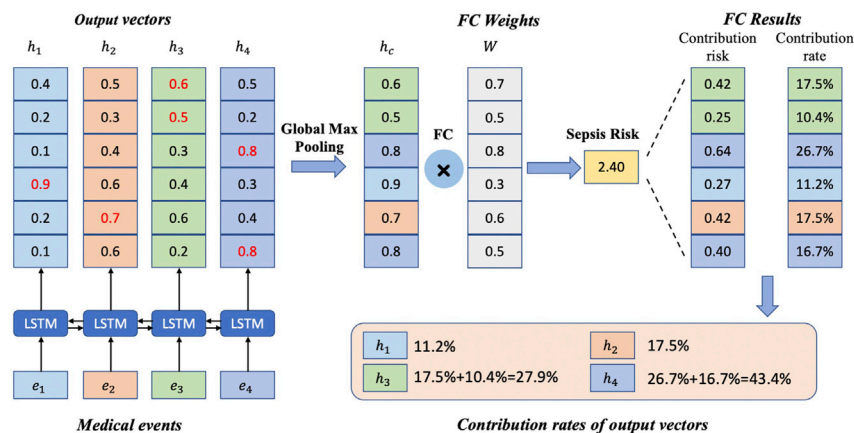


Figure 6. Interpretability of the proposed model with global max pooling: a toy example

Here we display four medical events (e_1, e_2, e_3, e_4) and their corresponding output vectors (h_1, h_2, h_3, h_4). After a global max pooling layer and a fully connected layer, the model predicts the risk of sepsis onset in the next 4 h for an individual patient. Each output vector’s contribution is then calculated by summing the corresponding dimensions’ contribution risks. Finally, the contribution of each medical event is calculated according to Equation 5.

To better align patient records at their last recorded medical event, the time of each event is mapped from $[0, T_{\text{lastevent}}]$ to $[-T_{\text{lastevent}}, 0]$.

LSTM and attention mechanism

RNNs are popular and suitable for sequential EHR data modeling. Given medical event embedding and time encoding vectors, we build our model based on LSTM³⁰ for its ability to recall long-term information. The LSTM model can be described as follows:

$$\begin{aligned}
 i_t &= \sigma(W_i \hat{e}_t + W_{it} \hat{p}_t + U_i h_{t-1} + b_i) \\
 f_t &= \sigma(W_f \hat{e}_t + W_{ft} \hat{p}_t + U_f h_{t-1} + b_f) \\
 o_t &= \sigma(W_o \hat{e}_t + W_{ot} \hat{p}_t + U_o h_{t-1} + b_o) \\
 C_t &= \sigma(W_{ce} \hat{e}_t + W_{ct} \hat{p}_t + U_c h_{t-1} + b_c) * i_t + C_{t-1} * f_t \\
 h_t &= o_t * \tanh(C_t)
 \end{aligned} \quad (Equation 2)$$

where σ is the sigmoid function, t denotes the t^{th} step of LSTM, and C_t is the corresponding cell state, and h_t is the output vector. \hat{e}_t is the input event embedding and \hat{p}_t is the input time encoding. $W_i, W_f, W_o, W_{ce} \in R^{k \times d}$, $W_{it}, W_{ft}, W_{ot}, W_{ct} \in R^{k \times 2d}$, $U_i, U_f, U_o, U_c \in R^{k \times d}$, and $b_i, b_f, b_o, b_c \in R^k$ are learnable parameters. Attention mechanism is used to automatically identify influential clinical features.

Global max pooling

RNN-based models are sometimes inefficient due to their long-term dependency. When the input sequence is too long, it is easy for the models to forget the earlier data. Therefore, we adopt a global pooling operation to shorten the distance between the earlier inputs and the final outputs. As is shown in Figure 3, all the outputs of the LSTM are concatenated, then a global pooling operation is followed. The output o_g is fed through the fully connected layer to produce the clinical risk of patient i , which is defined as

$$\begin{aligned}
 r_i &= W_s o_g + b_s \\
 y_i &= \sigma(r_i) \quad (Equation 3)
 \end{aligned}$$

where $W_s \in R^k$ and $b_s \in R$ are the learnable parameters and y_i denotes the predicted probability for sepsis onset. Because of the shortened distance between the inputs and the outputs, the pooling operation makes it more efficient to propagate the gradients. Besides, the global pooling operation is useful to compute the contribution rates of the outputs and their corresponding input medical events.

Objective function

For binary classification, the objective function is defined as the binary cross-entropy loss between ground truth y^* and predicted probability y :

$$L = -(y \log(y) + (1 - y) \log(1 - y)). \quad (\text{Equation 4})$$

Interpretability

Interpretability is very important for machine-learning models of clinical applications. The global pooling operation leveraged in our architecture can associate the contribution of each input medical event to the final clinical outcome, paving the way for interpretable clinical risk predictions.

In Figure 3, given the output vectors, the global max pooling operation is followed and produced the final patient feature vector h_c , which is used to predict risk of sepsis onset. We can track the output vectors which constitutes specific element of h_c . After the fully connected layer, we can calculate every dimension's contribution rate. For a case patient, the contribution rate of output vector h_t for the t^{th} input event is calculated as

$$c_t = \frac{h_t}{\sum_{j=1}^n \max(h_j, 0)}. \quad (\text{Equation 5})$$

To illustrate the interpretability of our model clearly, we display four input events and four corresponding six-dimensional output vectors (h_1, h_2, h_3, h_4) in Figure 6. Given patient feature vector (h_c) and fully connected parameters (W_s, b_s), the output risk is computed ($r_i = W_s h_c + b_s$). For example, the first dimension's contribution risk is 0.42 and the contribution rate is 17.5%, which comes from the third output vector h_3 . Similarly, the second dimension's contribution rate also comes from h_3 . Thus, the contribution rate of the third vector h_3 is computed by summing the two contribution rates. We thus compute the contribution rate of the input event e_3 as $c_3 = 17.5\% + 10.4\% = 27.9\%$. For feature j in event i , we can compute its contribution rate with attention weight as

$$c_{ij} = c_i * a_j. \quad (\text{Equation 6})$$

Implementation and evaluation

The four early-warning scores (MEWS, NEWS, SIRS, and qSOFA) are calculated based on the worst value for each physiological variable within the past 24 h before $T_{\text{onset}} - 4$ (i.e., the last observed time points). Logistic regression and random forest are implemented with the scikit-learn toolkit.³³ We implement gradient-boosting trees using LightGBM.³⁴ For the proposed LSTM-based model we use PyTorch,³⁵ and the number of time steps for LSTM is set to 100. For evaluation, 80% of the data are used for training, 10% for validation, and 10% for testing. The competition was hosted on Amazon Web Services, and experiments were conducted on a limited secure server to protect data privacy. GPUs are available to accelerate computing.

To evaluate the performance and discrimination of binary classifier, for each use case we use the AUC as the evaluation metric. The arithmetic average of AUC scores of two use cases is used for final performance comparison.

SUPPLEMENTAL INFORMATION

Supplemental information can be found online at <https://doi.org/10.1016/j.patter.2020.100196>.

ACKNOWLEDGMENTS

This work was supported by the National Institute on Aging (R03AG064379 for K.M.H., R01AG066749 for X.J.), the National Science Foundation (CBET-2037398 for C.Y. and P.Z.), the National Center for Advancing Translational Research (UL1TR002733 for P.Z.), the Cancer Prevention and Research Institute of Texas (RR180012 for X.J.), and a sponsored research agreement from Lyntek Medical Technologies Inc (for D.Z., C.Y., and P.Z.). The authors would like to thank Dr. Lawrence Lynn for the weekly discussions of sepsis during the 2019 DII National Data Science Challenge.

AUTHOR CONTRIBUTIONS

Conceptualization, P.Z.; Resources, X.J. (organizing the 2019 DII Challenge); Methodology, C.Y., D.Z., and P.Z.; Investigation, D.Z. and C.Y.; Formal Analysis, D.Z., C.Y., K.M.H., J.M.C., and P.Z.; Writing – Original Draft, D.Z., C.Y., and P.Z.; Writing – Review & Editing, D.Z., C.Y., K.M.H., X.J., J.M.C., and P.Z.; Supervision, P.Z.

DECLARATION OF INTERESTS

The authors declare no competing interests.

Received: October 11, 2020

Revised: November 3, 2020

Accepted: December 18, 2020

Published: January 19, 2021

REFERENCES

- Centers for Disease Control and Prevention (2016). Sepsis: data and reports. <https://www.cdc.gov/sepsis/datareports/index.html>.
- Torio, C.M., and Moore, B.J. (2016). National inpatient hospital costs: the most expensive conditions by payer, 2013. Healthcare Cost and Utilization Project (HCUP) Statistical Briefs. <https://www.hcup-us.ahrq.gov/reports/statbriefs/sb204-Most-Expensive-Hospital-Conditions.jsp>.
- Martin, G.S. (2012). Sepsis, severe sepsis and septic shock: changes in incidence, pathogens and outcomes. Expert Rev. Anti Infect. Ther. 10, 701–706. <https://doi.org/10.1016/j.afjem.2014.05.004>.
- Singer, M., Deutschman, C.S., Seymour, C.W., Shankar-Hari, M., Annane, D., Bauer, M., Bellomo, R., Bernard, G.R., Chiche, J.-D., Cooper-Smith, C.M., et al. (2016). The third international consensus definitions for sepsis and septic shock (sepsis-3). JAMA 315, 801–810. <https://doi.org/10.1001/jama.2016.0287>.
- Paoli, C.J., Reynolds, M.A., Sinha, M., Gittlin, M., and Crouser, E. (2018). Epidemiology and costs of sepsis in the United States—an analysis based on timing of diagnosis and severity level. Crit. Care Med. 46, 1889–1897. <https://doi.org/10.1097/CCM.0000000000003342>.
- Subbe, C.P., Kruger, M., Rutherford, P., and Gemmel, L. (2001). Validation of a modified early warning score in medical admissions. Q. J. Med 94, 521–526. <https://doi.org/10.1093/qjmed/94.10.521>.
- Smith, G.B., Prytherch, D.R., Meredith, P., Schmidt, P.E., and Featherstone, P.I. (2013). The ability of the national early warning score (NEWS) to discriminate patients at risk of early cardiac arrest, unanticipated intensive care unit admission, and death. Resuscitation 84, 465–470. <https://doi.org/10.1016/j.resuscitation.2012.12.016>.
- Bone, R.C., Balk, R.A., Cerra, F.B., Dellinger, R.P., Fein, A.M., Knaus, W.A., Schein, R.M., and Sibbald, W.J. (1992). Definitions for sepsis and organ failure and guidelines for the use of innovative therapies in sepsis. Chest 101, 1644–1655. <https://doi.org/10.1378/chest.101.6.1644>.
- Dorsett, M., Kroll, M., Smith, C.S., Asaro, P., Liang, S.Y., and Moy, H.P. (2017). qSOFA has poor sensitivity for prehospital identification of severe sepsis and septic shock. Prehosp. Emerg. Care 21, 489–497. <https://doi.org/10.1080/10903127.2016.1274348>.
- Usman, O.A., Usman, A.A., and Ward, M.A. (2019). Comparison of SIRS, qSOFA, and NEWS for the early identification of sepsis in the emergency department. Am. J. Emerg. Med. 37, 1490–1497. <https://doi.org/10.1016/j.ajem.2018.10.058>.
- Islam, M.M., Nasrin, T., Walther, B.A., Wu, C.-C., Yang, H.-C., and Li, Y.-C. (2019). Prediction of sepsis patients using machine learning approach: a meta-analysis. Comput. Methods Programs Biomed. 170, 1–9. <https://doi.org/10.1016/j.cmpb.2018.12.027>.
- Reyna, M.A., Josef, C.S., Jeter, R., Shashikumar, S.P., Westover, M.B., Nemat, S., Clifford, G.D., and Sharma, A. (2019). Early prediction of sepsis from clinical data: the PhysioNet/Computing in Cardiology Challenge 2019. 2019 computing in Cardiology (CinC). DOI: 10.23919/CinC49843.2019.9005736.
- Faisal, M., Scally, A., Richardson, D., Beatson, K., Howes, R., Speed, K., and Mohammed, M.A. (2018). Development and external validation of an automated computer-aided risk score for predicting sepsis in emergency medical admissions using the patient's first electronically recorded vital signs and blood test results. Crit. Care Med. 46, 612–618. <https://doi.org/10.1097/ccm.0000000000002967>.

14. Horng, S., Sontag, D.A., Halpern, Y., Jernite, Y., Shapiro, N.I., and Nathanson, L.A. (2017). Creating an automated trigger for sepsis clinical decision support at emergency department triage using machine learning. *PLoS One* 12, <https://doi.org/10.1371/journal.pone.0174708>.
15. Mollura, M., Mantoan, G., Romano, S., Lehman, L.-W., Mark, R.G., and Barbieri, R. (2020). The role of waveform monitoring in sepsis identification within the first hour of intensive care unit stay. In 2020 11th Conference of the European Study Group on Cardiovascular Oscillations (ESGCO). DOI: 10.1109/ESGCO49734.2020.9158013.
16. Kamaleswaran, R., Akbilgic, O., Hallman, M.A., West, A.N., Davis, R.L., and Shah, S.H. (2018). Applying artificial intelligence to identify physiologic markers predicting severe sepsis in the PICU. *Pediatr. Crit. Care Med.* 19, 495–503, <https://doi.org/10.1097/PCC.0000000000001666>.
17. Lyra, S., Leonhardt, S., and Antink, C.H. (2019). Early prediction of sepsis using random forest classification for imbalanced clinical data. In 2019 Computing in Cardiology (CinC). DOI: [10.23919/CinC49843.2019.9005769](https://doi.org/10.23919/CinC49843.2019.9005769).
18. Mao, Q., Jay, M., Hoffman, J.L., Calvert, J., Barton, C., Shimabukuro, D., Shieh, L., Chettipally, U., Fletcher, G., Kerem, Y., et al. (2018). Multicentre validation of a sepsis prediction algorithm using only vital sign data in the emergency department, general ward and ICU. *BMJ Open* 8, 017833, <https://doi.org/10.1136/bmjopen-2017-017833>.
19. Nemat, S., Holder, A., Razmi, F., Stanley, M.D., Clifford, G., and Buchman, T. (2018). An interpretable machine learning model for accurate prediction of sepsis in the ICU. *Crit. Care Med.* 46, 547–553, <https://doi.org/10.1097/CCM.0000000000002936>.
20. Miotto, R., Wang, F., Wang, S., Jiang, X., and Dudley, J.T. (2018). Deep learning for healthcare: review, opportunities and challenges. *Brief. Bioinformatics* 19, 1236–1246, <https://doi.org/10.1093/bib/bbx044>.
21. Kam, H.J., and Kim, H.Y. (2017). Learning representations for the early detection of sepsis with deep neural networks. *Comput. Biol. Med.* 89, 248–255, <https://doi.org/10.1016/j.compbiomed.2017.08.015>.
22. Choi, E., Schuetz, A., Stewart, W.F., and Sun, J. (2016a). Using recurrent neural network models for early detection of heart failure onset. *J. Am. Med. Inform. Assoc.* 24, 361–370, <https://doi.org/10.1093/jamia/ocw112>.
23. Che, Z., Purushotham, S., Cho, K., Sontag, D., and Liu, Y. (2018). Recurrent neural networks for multivariate time series with missing values. *Sci. Rep.* 8, 1–12, <https://doi.org/10.1038/s41598-018-24271-9>.
24. Choi, E., Bahadori, M.T., Sun, J., Kulas, J., Schuetz, A., and Stewart, W. (2016b). RETAIN: an interpretable predictive model for healthcare using reverse time attention mechanism. In *Advances in Neural Information Processing Systems*, vol. 29, D. Lee, M. Sugiyama, U. Luxburg, I. Guyon, and R. Garnett, eds., pp. 3504–3512. <https://proceedings.neurips.cc/paper/2016/file/231141b34c82aa95e48810a9d1b33a79-Paper.pdf>.
25. Ma, F., Chitta, R., Zhou, J., You, Q., Sun, T., and Gao, J. (2017). Dipole: diagnosis prediction in healthcare via attention-based bidirectional recurrent neural networks. In *Proceedings of the 23rd ACM SIGKDD International Conference on Knowledge Discovery and Data Mining. KDD '17*. pp. 1903–1911. DOI: 10.1145/3097983.3098088.
26. Sakr, Y., Jaschinski, U., Wittebole, X., Szakmany, T., Lipman, J., Namendys Silva, S.A., Martin-Loeches, I., Leone, M., Lupu, M.-N., and Vincent, J.-L.; ICON Investigators (2018). Sepsis in intensive care unit patients: worldwide data from the intensive care over nations audit. *Open Forum Infect. Dis.* 5, ofy313, <https://doi.org/10.1093/ofid/ofy313>.
27. Taylor, R.A., Pare, J.R., Venkatesh, A.K., Mowafi, H., Melnick, E.R., Fleischman, W., and Hall, M.K. (2016). Prediction of in-hospital mortality in emergency department patients with sepsis: a local big data-driven, machine learning approach. *Acad. Emerg. Med.* 23, 269–278, <https://doi.org/10.1111/acem.12876>.
28. Levy, M.M., Fink, M.P., Marshall, J.C., Abraham, E., Angus, D., Cook, D., Cohen, J., Opal, S.M., Vincent, J.-L., and Ramsay, G. (2003). 2001 SCCM/ESICM/ACCP/ATS/SIS international sepsis definitions conference. *Intensive Care Med.* 29, 530–538, <https://doi.org/10.1007/s00134-003-1662-x>.
29. Cho, K., van Merriënboer, B., Bahdanau, D., and Bengio, Y. (2014). On the properties of neural machine translation: encoder–decoder approaches. In *Proceedings of SSST-8, Eighth Workshop on Syntax, Semantics and Structure in Statistical Translation*. pp. 103–111. DOI: [10.3115/v1/W14-4012](https://doi.org/10.3115/v1/W14-4012).
30. Hochreiter, S., and Schmidhuber, J. (1997). Long short-term memory. *Neural Comput.* 9, 1735–1780, <https://doi.org/10.1162/neco.1997.9.8.1735>.
31. Yin, C., Zhao, R., Qian, B., Lv, X., and Zhang, P. (2019). Domain knowledge guided deep learning with electronic health records. In 2019 IEEE International Conference on Data Mining (ICDM). pp. 738–747. DOI: [10.1109/ICDM.2019.00084](https://doi.org/10.1109/ICDM.2019.00084).
32. Vaswani, A., Shazeer, N., Parmar, N., Uszkoreit, J., Jones, L., Gomez, A.N., Kaiser, Ł., and Polosukhin, I. (2017). Attention is all you need. In *Advances in Neural Information Processing Systems 30 (NIPS 2017)*, pp. 5998–6008, <https://doi.org/10.5555/3295222.3295349>.
33. Pedregosa, F., Varoquaux, G., Gramfort, A., Michel, V., Thirion, B., Grisel, O., Blondel, M., Prettenhofer, P., Weiss, R., Dubourg, V., et al. (2011). Scikit-learn: machine learning in Python. *J. Machine Learn. Res.* 12, 2825–2830, <https://doi.org/10.5555/1953048.2078195>.
34. Ke, G., Meng, Q., Finley, T., Wang, T., Chen, W., Ma, W., Ye, Q., and Liu, T.-Y. (2017). Lightgbm: a highly efficient gradient boosting decision tree. In *Advances in Neural Information Processing Systems 30 (NIPS 2017)*, pp. 3146–3154, <https://doi.org/10.5555/3294996.3295074>.
35. Paszke, A., Gross, S., Massa, F., Lerer, A., Bradbury, J., Chanan, G., Killeen, T., Lin, Z., Gimelshein, N., Antiga, L., et al. (2019). PyTorch: an imperative style, high-performance deep learning library. In *Advances in Neural Information Processing Systems 32 (NeurIPS 2019)*, pp. 8024–8035. <https://papers.nips.cc/paper/2019/file/bdbca288fee792f2bfa9f7012727740-Paper.pdf>.

PATTER, Volume 2

Supplemental Information

An interpretable deep-learning model for early prediction of sepsis in the emergency department

Dongdong Zhang, Changchang Yin, Katherine M. Hunold, Xiaoqian Jiang, Jeffrey M. Caterino, and Ping Zhang

1. Supplemental Figures

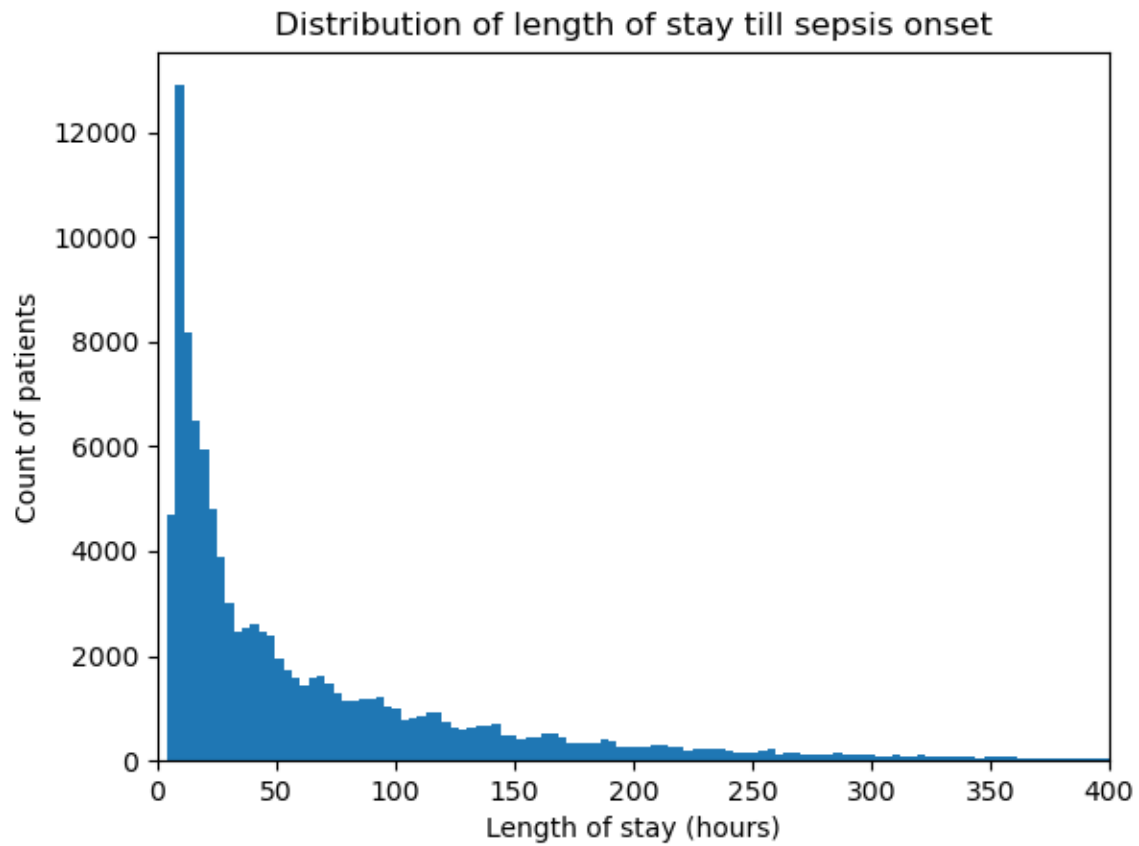


Figure S1. Distribution of length of stay from admission to sepsis onset on the dataset.

2. Supplemental Tables

Table S1. Feature summarization and description of 2019 DII challenge dataset.

Feature	Unit	Missing rate	Contribution rate	Description
A/G Ratio	NULL	0.995	0	Albumin / Globulin Ratio
Albumin Quant	g/dL	0.983	0.001	Albumin Quantitative, Serum
Alk Phos, Serum	U/L	0.985	0.001	Alkaline Phosphatase, Serum
ALT/SGPT	U/L	0.984	0.001	Alanine Aminotransferase / SGPT
Amylase, Serum	U/L	0.969	0.002	Amylase, Serum Enzymatic Activity/Volume
Anion Gap	mmol/L	0.969	0.001	Anion Gap
AST/SGOT	U/L	0.983	0.001	Aspartate Aminotransferase / SGOT
Base Excess	mmol/L	0.98	0.001	Base Excess
Baso %	%	0.97	0.001	Basophils Percent
Baso Abs	10*3/uL	0.987	0.002	Basophils Absolute Count
Baso Abs Cnt Bld	10*3/uL	0.989	0.001	Basophils Absolute Count Blood
Bilirubin Direct, Serum	mg/dL	0.997	0.002	Bilirubin Direct Quantitative, Serum
Bilirubin Serum Quant	mg/dL	0.997	0.001	Bilirubin Total Quantitative, Serum
Bilirubin Total Bld mCnc	mg/dL	0.988	0.001	Bilirubin Total Serum or Plasma Mass/Volume
Blood Urea Nitrogen	mg/dL	0.958	0.001	Blood Urea Nitrogen
BMI	NULL	0.978	0.002	BMI, Body Mass Index
BNP-B Type Natriuretic Peptide	pg/mL	0.999	0.002	BNP-B Type Natriuretic Peptide
Body Surface Area	m2	0.988	0.004	Body Surface Area
Braden Scale	NULL	0.917	0.024	Braden Q Scale
BUN/Creat Ratio	NULL	0.99	0.002	Blood Urea Nitrogen Creatinine Ratio
Calcium Ionized	mmol/L	0.993	0.001	Calcium Ionized
Calcium Quant	mg/dL	0.959	0.001	Calcium Quantitative, Blood
Chol HDL	mg/dL	0.999	0.001	HDL Cholesterol
Chol Total, Serum	mg/dL	0.999	0.002	Cholesterol Total, Serum
CK/CPK, Total, Serum	U/L	0.997	0.005	CK/CPK, Total, Serum
CKMB	ng/mL	0.998	0.001	Creatine Kinase-MB
Cl, Serum	mmol/L	0.959	0.002	Chloride, Serum
CO2	mmol/L	0.912	0.011	Carbon dioxide
Creatinine, Serum Quant	mg/dL	0.958	0.002	Creatinine, Serum Quantitative
DBP	mm[Hg]	0.278	0.164	Blood Pressure Diastolic
Diff Bands	%	0.996	0.001	Differential Bands
Diff Bands, Abs	/uL	0.999	0	Diff Bands, Abs
Diff Blast	K/mm3	0.999	0	Differential Blast
Diff, Eosinophil %	%	0.98	0.001	Eosinophil Percent
Diff, Eosinophil Abs Quant Bld	10*3/uL	0.987	0.001	Eosinophil Absolute Count Blood
Diff, Eosinophil Count %	%	0.989	0.007	Diff, Eosinophil Count %
Diff, Eosinophil Count, Abs	K/mm3	0.988	0.006	Diff, Eosinophil Count, Abs
Diff, Granulocyte %	%	0.994	0.004	Granulocyte Percent
Diff Nucleated RBC	%	0.994	0	Differential Nucleated Red Blood Cell (RBC)
ETCO2	mm[Hg]	0.963	0.004	ETCO2 (End Tidal CO2)

FiO2	%	0.917	0.054	FiO2 (Fraction of Inspired Oxygen)
FLACC Pain Scale	NULL	0.99	0.013	FLACC Pain Scale (Face Legs Arms Cry Consolability Scale)
GFR/BSA Pred Black SerPl MDRD ArVRat	mL/min/1.73m ²	0.992	0.002	Glomerular Filtration Rate/1.73 sq M Predicted Among Blacks Creatinine Based Formula (MDRD)
GFR/BSA Pred non black SerPl MDRD ArVRat	mL/min	0.994	0.002	Glomerular Filtration Rate/1.73 sq M Predicted Among non-blacks Creatinine Based Formula (MDRD)
Glasgow Coma Score	NULL	0.728	0.086	Glasgow Coma Score
Globulin, Serum	g/dL	0.996	0	Globulin, Serum
Glomerular Filtration Rate	mL/min/1.73m ²	0.972	0.004	Glomerular Filtration Rate
Glucose, Serum Quant	mg/dL	0.95	0.014	Glucose, Serum/Plasma Quantitative
Glucose Stick/Meter WBlood POC	mg/dL	0.944	0.13	Glucose Stick/Meter Whole Blood POC
HCO3	mmol/L	0.97	0.002	HCO3
Hct	%	0.956	0.002	Hematocrit
Height	cm	0.973	0.001	Height
Hgb	g/dL	0.954	0.003	Hemoglobin
Hgb A1C	%	0.999	0.003	Hemoglobin A1C (Glycosylated Hemoglobin)
HR	bpm	0.288	0.206	Heart Rate
Imm Granulocytes Cnt Bld Auto, %	%	0.998	0.004	Imm Granulocytes Cnt Bld Auto, %
Imm Granulocytes Cnt Bld Auto, Abs	10 ³ /uL	0.998	0.001	Imm Granulocytes Cnt Bld Auto, Abs
INR Platelet Poor Plasma	NULL	0.997	0.001	INR Platelet Poor Plasma
International Normalized Ratio	NULL	0.988	0.004	International Normalized Ratio
Iron, Serum	ug/dL	0.999	0.004	Iron, Serum
Lactic Acid Blood	mmol/L	0.994	0.002	Blood Gas Lactic Acid Blood
Lactic Dehydrogenase	U/L	0.999	0.008	Lactic Dehydrogenase
Lipase, Serum	U/L	0.998	0.001	Lipase, Serum
Lymph %	%	0.968	0.002	Lymphocyte Percent
Lymph Abs Cnt	10 ³ /uL	0.969	0.002	Lymphocyte Absolute Count
Magnesium, Serum/Plasma	mg/dL	0.977	0.002	Magnesium, Serum/Plasma
MAP	mm[Hg]	0.511	0.135	Mean airway pressure (MAP)
MCH Concentration	g/dL	0.96	0.002	MCH Concentration
Mean Corpuscular Hemoglobin	pg	0.96	0.001	Mean Corpuscular Hemoglobin
Mean Corpuscular Volume	fL	0.96	0.002	Mean Corpuscular Volume
Mean Platelet Volume	fL	0.964	0.002	Mean Platelet Volume
Mono %	%	0.966	0.003	Monocyte Percent
Mono Abs Cnt Bld	10 ³ /uL	0.97	0.001	Monocyte Absolute Count Blood
Neutrophil %	%	0.974	0.001	Neutrophil Percent
Neutrophil Abs Bld Cnt	10 ³ /uL	0.974	0	Neutrophil Absolute Count Blood
Pain Score	NULL	0.841	0.133	Pain Scale Score
PCO2	mm[Hg]	0.964	0.006	Partial Pressure Carbon Dioxide (PCO2)
Peak inspiratory pressure	cmH20	0.959	0.002	Peak inspiratory pressure
Peep	cmH20	0.939	0.002	Peep (Positive End Expiratory Pressure)

pH, Arterial	pH units	0.971	0.001	pH, Arterial
Phosphorus, Serum	mg/dL	0.982	0.002	Phosphorus, Serum
pH, Urine	pH units	0.998	0.003	pH, Urine
Platelet Count	10 ³ /uL	0.961	0	Platelet Count
PO2	mm[Hg]	0.968	0.002	Partial Pressure of Oxygen (PO2)
Potassium, Serum	mmol/L	0.955	0.002	Potassium, Serum
Protein Total, Serum	g/dL	0.985	0.001	Protein Total, Serum
PT	s	0.985	0.002	Prothrombin Time
PTT	s	0.99	0.008	Partial Thromboplastin Time
PTT/APTT PPP	s	0.997	0.004	PTT/APTT, Platelet Poor Coagulation Assay
Pulse	bpm	0.796	0.084	Pulse
Pulse Oximetry	%	0.982	0.011	Pulse Oximetry
QRS Duration	s	0.984	0.013	QRS Duration
QT Interval	s	0.982	0.038	QT Interval
RBC	10 ⁶ /uL	0.961	0.001	Red Blood Cell Count
Red Blood Cell Distribution Width	%	0.966	0.001	Red Blood Cell Distribution Width
Resp Rt	Br/min	0.22	0.158	Respiratory Rate
SBP	mm[Hg]	0.335	0.117	Blood Pressure Systolic
SO2	%	0.58	0.07	O2 Saturation (SO2)
Sodium, Serum	mmol/L	0.958	0.001	Sodium, Serum
Specific Gravity Urine	NULL	0.998	0.002	Specific Gravity, Urine
TCO2	mmol/L	0.991	0.015	Carbon dioxide Total (TCO2)
Temp	Cel	0.668	0.143	Temperature (Route Not Specified)
Thyroid Stimulating Hormone	u[iU]/mL	0.998	0.003	Thyroid Stimulating Hormone
Tidal Volume	mL	0.956	0.004	Tidal Volume
Triglyceride, Serum	mg/dL	0.998	0.001	Triglyceride, Serum
Troponin I	ng/mL	0.997	0.002	Troponin I
Troponin T S/Pl	ng/mL	0.999	0.001	Troponin T, Serum/Plasma
UA Red Blood Cell	[HPF]	0.999	0.005	UA Red Blood Cell
UA Urobilinogen	mg/dL	0.999	0.003	UA Urobilinogen
UA WBC	[HPF]	0.998	0.002	UA White Blood Cell
Vitamin B12, Serum	pg/mL	0.999	0.003	Vitamin B12, Serum Quantitative (Cobalamin)
WBC	10 ³ /uL	0.96	0.001	White Blood Cell Count
Weight	kg	0.964	0.008	Weight

Table S2. P-value matrix of model performance (AUC) across various subpopulations on Case1 sepsis prediction.

		Gender		Race				Age group							
		Female	Male	African American	Asian	Caucasian	Others/ unknown	20~30	30~40	40~50	50~60	60~70	70~80	<20	>=80
Gender	Female	1	0.025	0.33	0.22	0.02	0.012	0.046	0.007	0.64	0.123	0.323	0.011	0.013	0.856
	Male	0.025	1	0.01	0.478	0.747	0.165	0.314	0.081	0.005	0.582	0.624	0.112	0.002	0.075
Race	African American	0.33	0.01	1	0.138	0.008	0.005	0.019	0.004	0.501	0.037	0.118	0.005	0.046	0.299
	Asian	0.22	0.478	0.138	1	0.504	0.724	0.775	0.831	0.182	0.417	0.405	0.849	0.027	0.244
	Caucasian	0.02	0.747	0.008	0.504	1	0.221	0.366	0.109	0.004	0.464	0.546	0.143	0.002	0.06
	Others/ unknown	0.012	0.165	0.005	0.724	0.221	1	0.902	0.67	0.004	0.135	0.217	0.657	0.001	0.026
Age group	20~30	0.046	0.314	0.019	0.775	0.366	0.902	1	0.85	0.025	0.24	0.274	0.824	0.003	0.068
	30~40	0.007	0.081	0.004	0.831	0.109	0.67	0.85	1	0.003	0.074	0.137	0.956	0.001	0.016
	40~50	0.64	0.005	0.501	0.182	0.004	0.004	0.025	0.003	1	0.044	0.192	0.005	0.017	0.552
	50~60	0.123	0.582	0.037	0.417	0.464	0.135	0.24	0.074	0.044	1	0.885	0.093	0.003	0.221
	60~70	0.323	0.624	0.118	0.405	0.546	0.217	0.274	0.137	0.192	0.885	1	0.148	0.008	0.423
	70~80	0.011	0.112	0.005	0.849	0.143	0.657	0.824	0.956	0.005	0.093	0.148	1	0.001	0.022
	<20	0.013	0.002	0.046	0.027	0.002	0.001	0.003	0.001	0.017	0.003	0.008	0.001	1	0.014
	>=80	0.856	0.075	0.299	0.244	0.06	0.026	0.068	0.016	0.552	0.221	0.423	0.022	0.014	1